Cellular/Molecular

Synaptic Vesicle Generation from Activity-Dependent Bulk Endosomes Requires Calcium and Calcineurin

Giselle Cheung and Michael A. Cousin
Centre for Integrative Physiology, University of Edinburgh, Edinburgh EH8 9XD, United Kingdom

Activity-dependent bulk endocytosis (ADBE) is the dominant mode of synaptic vesicle (SV) endocytosis during high-frequency stimulation in central nerve terminals. ADBE generates endosomes direct from the plasma membrane, meaning that high concentrations of calcium will be present in their interior due to fluid phase uptake from the extracellular space. Morphological and fluorescent assays were used to track the generation of SVs from bulk endosomes in primary neuronal culture. This process was functionally uncoupled from both SV exocytosis and plasma membrane retrieval events by intervening only after SV fusion and endocytosis were completed. Either intracellular (BAPTA-AM) or intra-endosomal (Rhod-dextran) calcium chelation inhibited SV generation from bulk endosomes, indicating that calcium efflux from this compartment is critical for this process. The V-type ATPase antagonist bafilomycin A1 also arrested SV generation from bulk endosomes, indicating endosomal acidification may be required for calcium efflux. Finally, pharmacological inhibition of the calcium-dependent protein phosphatase calcineurin blocked endosomal SV generation, identifying it as a key downstream effector in this process. These results reveal a novel and key role for the fluid phase uptake of extracellular calcium and its subsequent efflux in the SV lifecycle.

Introduction

The local generation of synaptic vesicles (SVs) after exocytosis at central nerve terminals is critical for the maintenance of neurotransmission across a wide range of stimuli. Two major modes of SV retrieval exist in nerve terminals: clathrin-mediated endocytosis (CME) and activity-dependent bulk endocytosis (ADBE). CME is the dominant SV retrieval mode during mild stimulation (Granseth et al., 2006; Zhu et al., 2009), whereas during stronger stimulation ADBE is triggered to supply additional retrieval capacity (Richards et al., 2000; Clayton et al., 2008). ADBE is tightly coupled to neuronal activity and immediately corrects for changes in the nerve terminal surface area, forming endosomes directly from the plasma membrane. SVs then bud from these bulk endosomes in a clathrin- and adaptor protein-dependent manner (Heerssen et al., 2008; Kasprowicz et al., 2008; Cheung and Cousin, 2012).

SVs generated via endocytosis replenish the recycling pool of SVs, defined as those mobilized during neuronal activity (Kim and Ryan, 2010). The recycling pool can be subdivided into the readily releasable pool (RRP), which is immediately mobilized during stimulation, and the reserve pool, which is mobilized only during intense stimulation (Rizzoli and Betz, 2005). ADBE-derived SVs selectively replenish the reserve pool (Richards et al., 2000; Cheung et al., 2010; Cheung and Cousin, 2012), suggesting reserve pool replenishment and triggering of ADBE are linked to the same stimulus.

ADBE is tightly coupled to neuronal activity and is dependent on the activation of the calcium/calmodulin-dependent protein phosphatase calcineurin (Clayton et al., 2009; Wu et al., 2009). During intense stimulation, calcineurin dephosphorylates the large GTPase dynamin I, allowing an interaction with the F-BAR protein syndapin (Anggono et al., 2006). Both events are essential for ADBE to proceed (Clayton et al., 2009). Therefore, activity-dependent influx of extracellular calcium is essential for ADBE to occur.

During ADBE, extracellular calcium should also be accumulated inside bulk endosomes by fluid phase uptake; however, the potential role of this calcium store in the SV life cycle has not been investigated. Using newly validated morphological and functional assays, we tracked the generation of SVs from bulk endosomes by uncoupling this process from both SV exocytosis and plasma membrane retrieval events. We show that extracellular calcium, which was accumulated inside bulk endosomes, is essential for the generation of SVs from these structures, uncovering a novel and essential calcium-dependent stage in the SV life cycle.

Materials and Methods

FM1-43, TMR-dextran, Rhod-dextran, fura-2-AM, penicillin/streptomycin, phosphate-buffered salts, fetal calf serum, and Minimal Essential Medium were purchased from Invitrogen. BAPTA-AM was from Tocris Bioscience. Glutaraldehyde and osmium tetroxide were from Agar Scientific. Bafilomycin A1 was from Acros Organics. All other reagents were from Sigma.

Labeling of endocytic pathways by horseradish peroxidase. Rat cerebellar granule neuron cultures were prepared as previously described (Clayton

Received Oct. 4, 2012; revised Dec. 10, 2012; accepted Jan. 7, 2013.

Author contributions: M.A.C. designed research; G.C. performed research; G.C. analyzed data; G.C. and M.A.C. wrote the paper.

This work was supported by Grant 084277 from the Wellcome Trust. We thank Dr. Alan Prescott and Mr. John James (both from University of Dundee) for excellent technical assistance.

The authors declare no competing financial interests.

Correspondence should be addressed to Michael A. Cousin, Membrane Biology Group, Centre for Integrative Physiology, George Square, University of Edinburgh, Edinburgh EH8 9XD, United Kingdom. E-mail: M.Cousin@ed.ac.uk.

DOI:10.1523/JNEUROSCI.4697-12.2013

 0270-6474/13/333370-10$15.00/0

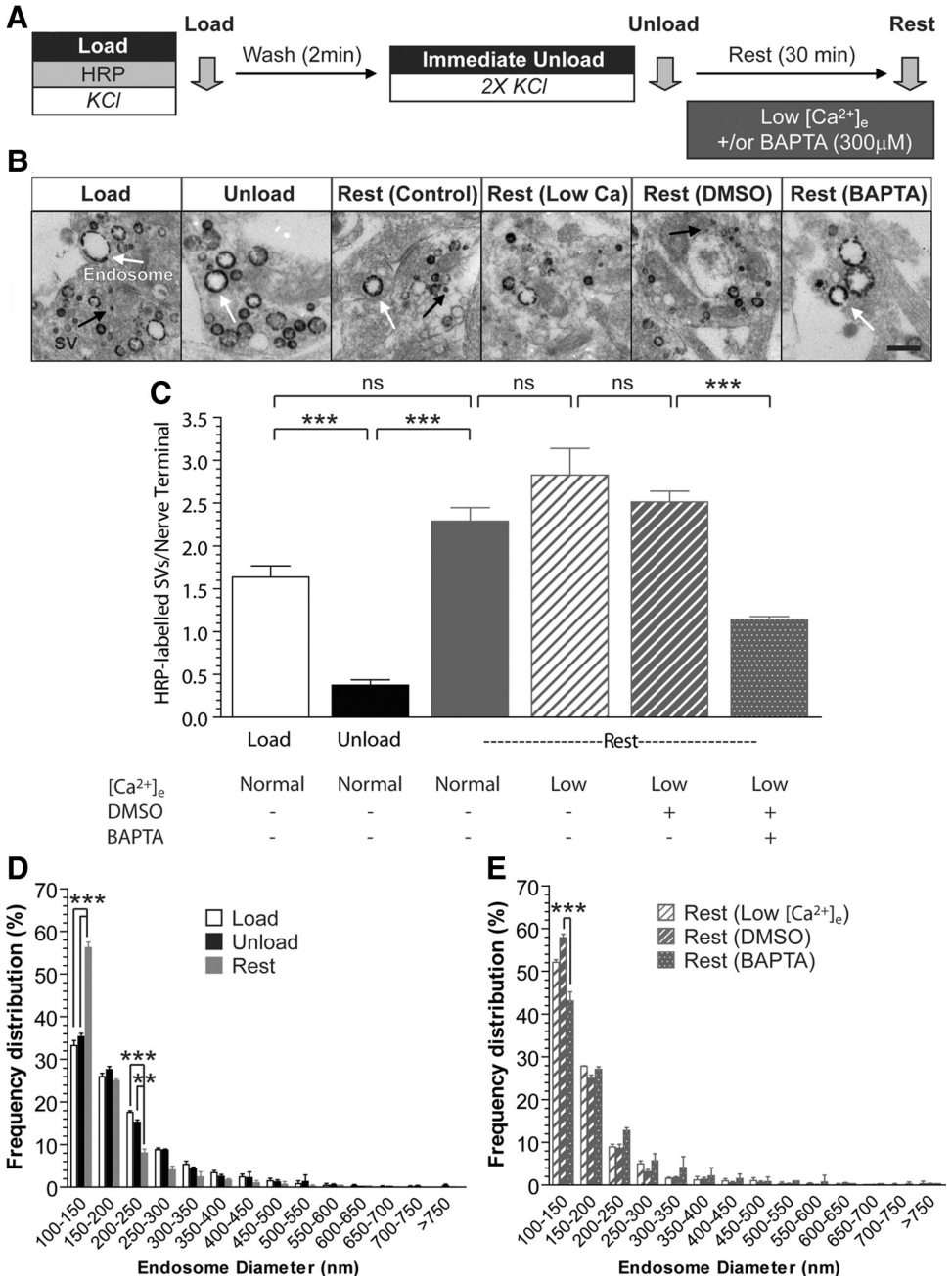

Figure 1. SV budding from bulk endosomes requires intracellular calcium. ***A***, Cultures were loaded with HRP (10 mg/ml) for 2 min in the presence of KCl (50 mM) and washed immediately to remove excess HRP. Cells were then stimulated twice with KCl (50 mM, 30 s each) to release all available SVs (Immediate Unload) and left to rest for 30 min. Where indicated, cultures were incubated in the presence of low extracellular calcium (Low $[Ca^{2+}]_e$) after the immediate unload, with some solutions supplemented with either BAPTA-AM (300 μM) or a DMSO vehicle control. Cultures were fixed after HRP loading (Load), the immediate unload (Unload), or the rest period (Rest), as indicated by arrows. ***B***, Representative electron micrographs of the treatments described above are shown. Scale bar, 500 nm. Black and white arrows indicate HRP-labeled SVs and endosomes, respectively. ***C***, Bar graph displays the mean number of HRP-labeled SVs per nerve terminal ± SEM in either 1.3 mM extracellular calcium (Normal) or low $[Ca^{2+}]_e$ (number of independent experiments: Load, 4; Unload, 3; Rest, 4; Rest-Low $[Ca^{2+}]_e$, 3; Rest-DMSO, 3; Rest-BAPTA, 3; $^{***}p < 0.001$, one-way ANOVA). ***D***, ***E***, Frequency distribution of endosome diameter for Load, Unload, and Rest in normal extracellular calcium conditions (***D***) or Rest for Low $[Ca^{2+}]_e$-, DMSO-, and BAPTA-treated conditions (***E***). At least 70 HRP-labeled endosomes were used for diameter measurements per independent experiment ($^{**}p < 0.01$, $^{***}p < 0.001$, two-way ANOVA for ***D*** and ***E***).

et al., 2009). Cultures were fixed and processed for electron microscopy as described previously (Cheung et al., 2010). Briefly, cultures were placed in incubation medium [in mM: 170 NaCl, 3.5 KCl, 0.4 KH_2PO_4, 20 TES (*N*-tris[hydroxyl-methyl]-methyl-2-aminoethane-sulfonic acid), 5 $NaHCO_3$, 5 glucose, 1.2 Na_2SO_4, 1.2 $MgCl_2$, and 1.3 $CaCl_2$, pH 7.4] for 10 min and then stimulated for 2 min with 50 mM KCl in the presence of 10 mg/ml horseradish peroxidase (HRP). After washout of HRP, cultures were immediately stimulated with two consecutive 30 s applications of 50 mM KCl. Cultures were then left to rest for 30 min. Cultures were incubated with pharmacological antagonists or dextrans during the load, unload, or rest period. In some cases, cultures were incubated with a low calcium medium, which differed from incubation medium by decreasing $CaCl_2$ to 50 μM, raising $MgCl_2$ to 10 mM, and adding 100 μM EGTA. Cultures were fixed in 2% glutaraldehyde in phosphate-buffered saline at one of the three fixation time points: directly after HRP loading, after unloading, or after the 30 min rest period. After washing with 100 mM Tris, pH 7.4, cultures were exposed to 0.1% diaminobenzidine and 0.2% H_2O_2 in 100 mM Tris until color developed. Cultures were then washed with 100 mM Tris, stained with 1% osmium tetroxide for 30 min, and then dehydrated using an ethanol series and polypropylene oxide and

embedded using Durcupan. Samples were sectioned, mounted on grids and viewed using an FEI Tecnai 12 transmission electron microscope. Nerve terminals were included in the analysis providing they contained small SVs, regardless of whether they contained HRP. Intracellular structures that were <100 nm in diameter were arbitrarily designated to be SVs, whereas larger structures were considered to be endosomes. The average endosome diameter was obtained by taking the average of the longest and shortest diameters of individual endosomes using ImageJ (National Institutes of Health).

Fluorescence imaging of SV pool replenishment. Fluorescence imaging of SV pool replenishment was performed as previously described (Cheung and Cousin, 2012). Briefly, cultures were repolarized for 10 min in incubation medium and then mounted in an imaging chamber (RC-21BRFS, Warner Instruments). Invaginating membrane was loaded with FM1-43 (10 μM) by evoking SV turnover using electrical field stimulation delivered using platinum wires embedded in the imaging chamber (800 action potentials at 80 Hz, 100 mA, 1 ms pulse width). After washout of excess FM dye, cultures were immediately stimulated (called Immediate Unload) with sequential trains of action potentials to first unload the RRP (30 Hz for 2 s) and then the reserve pool (three trains of 40 Hz for 10 s). After a 30 min rest period, an identical unloading protocol was repeated (called Second Unload). This protocol allows quantification of newly generated SVs that replenish the RRP and reserve pool. The average fluorescence drop for each unloading step was expressed as a percentage of the total SV recycling pool (RRP plus reserve pool) of the Immediate Unload, allowing comparison across multiple experiments.

In all experiments, fluorescence signals were visualized using a Zeiss AxioObserver A1 epifluorescence microscope. FM dye loading and unloading were monitored at 500 nm excitation (in all cases, emission was >535 nm) using a 20× air objective. All images were acquired using a Zeiss AxioCam CCD Camera controlled by Zeiss AxioVision Rel. software. Time-lapse FM images were acquired at 4 s intervals.

Monitoring of intracellular free calcium. Cultures were repolarized for 10 min in incubation medium and then loaded with 10 μM fura-2/AM for 30 min. Cultures were then washed three times and mounted in an imaging chamber (RC-21BRFS, Warner Instruments). Cultures were then exposed to 300 μM BAPTA-AM for different amounts of time (0, 2, 5, or 10 min) before stimulation with a train of 800 action potentials at 40 Hz. Increases in $[Ca^{2+}]_i$ were calculated by monitoring fluorescence changes at defined regions of interest at both 340 and 380 nm excitation and emission of >505 nm. The $[Ca^{2+}]_i$ response was calibrated using the Grynkiewicz equation (Grynkiewicz et al., 1985), where R_{max} was obtained by exposure to 5 μM ionomycin to equalize calcium across the membrane and R_{min} was obtained by subsequent incubation with 15 mM EGTA.

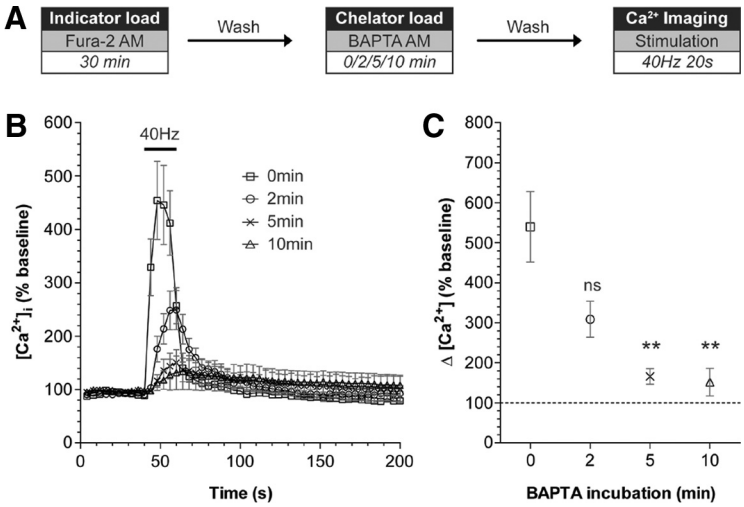

Figure 2. Chelation of intracellular calcium using BAPTA-AM. ***A***, Cultures were loaded with the calcium indicator Fura-2 AM (10 μM) for 30 min. BAPTA-AM (300 μM) was then added for either 0, 2, 5, or 10 min respectively. After washing, the intracellular calcium concentration $[Ca^{2+}]_i$ was monitored over time. The ability of BAPTA to chelate intracellular calcium was assessed by challenging cultures with a train of 800 action potentials (40 Hz). ***B***, Representative traces in $[Ca^{2+}]_i$ are shown for cells incubated with BAPTA for the indicated time periods. Bar indicates the period of stimulation. ***C***, The mean $[Ca^{2+}]_i$ increase in response to stimulation is plotted ±SEM (number of independent experiments: 0 min, 5; 2 min, 3; 5 min, 4; 10 min, 4; $^{**}p < 0.01$, one-way ANOVA compared with 0 min BAPTA incubation.

Results

SV budding from bulk endosomes is calcium dependent

The generation of bulk endosomes by ADBE involves fluid phase uptake of the extracellular milieu. Calcium is present at millimolar concentrations in the extracellular space; therefore, it should initially be present at this molarity inside bulk endosomes. To determine whether this endosomal store of calcium impacted on SV generation during ADBE, we performed a series of simple morphological experiments in primary neuronal cultures using a recently validated uptake assay (Cheung and Cousin, 2012).

To observe SV generation from bulk endosomes specifically, both CME and ADBE were triggered using a maximal depolarizing stimulus (50 mM KCl) in the presence of the fluid-phase marker HRP (Fig. 1*A*). In this assay, SVs and bulk endosomes that were generated by CME and ADBE, respectively, are visible as HRP-labeled structures (Fig. 1*B*). To visualize the generation of new SVs from HRP-labeled bulk endosomes, existing HRP-labeled SVs were depleted using two sequential stimuli of 50 mM KCl (Fig. 1 *B*, *C*). After a 30 min rest period, new HRP-labeled SVs appear in nerve terminals (Fig. 1*A*–*C*), which originate from bulk endosomes, since these structures are the only remaining source of HRP. In agreement, the production of new HRP-labeled SVs occurred in parallel with the appearance of smaller HRP-labeled endosomes (Fig. 1*D*). Therefore, this protocol allows tracking of HRP-labeled SVs specifically generated from bulk endosomes during a defined time window (Cheung and Cousin, 2012).

To determine whether SV generation from bulk endosomes was calcium dependent, we used the intracellular calcium chelator BAPTA-AM. We hypothesized that application of this chelator should inhibit SV budding if increased intracellular calcium was required for this event to occur, since BAPTA has both a high affinity and fast on-rate for calcium binding. To ensure that SV budding was decoupled from bulk endosome generation, BAPTA-AM (300 μM) was applied only after the completion of ADBE and depletion of HRP-labeled SVs (Fig. 1*A*). Acute application of this concentration of BAPTA-AM can buffer intracellular free calcium ($[Ca^{2+}]_i$) increases within 2 min (Fig. 2). To ensure that any observed effect on SV generation was due to intracellular calcium, BAPTA-AM was applied in the presence of low extracellular calcium. BAPTA-AM significantly reduced the generation of new HRP-labeled SVs from bulk endosomes, whereas exposure to either low extracellular calcium alone or a vehicle control had no effect (Fig. 1*C*). In addition, BAPTA-AM-treated neurons possessed fewer small endosomes after the 30 min rest period when compared against vehicle control conditions, again indicative of an inhibition of SV budding (Fig. 1*E*). Thus, an increase in $[Ca^{2+}]_i$ is required for SV budding from bulk endosomes.

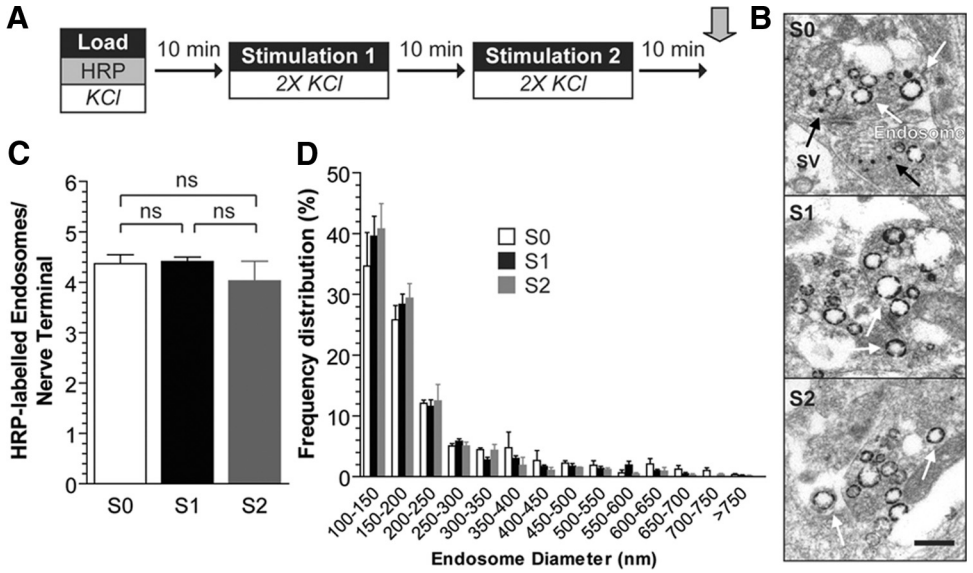

Figure 3. SV budding from bulk endosomes is independent of neuronal activity. ***A***, Cultures were loaded with HRP (10 mg/ml) for 2 min in the presence of KCl (50 mM) and washed immediately to remove excess HRP. Cells were then left to rest for 30 min, after which point they were fixed as indicated by arrow. Where indicated, two KCl stimulations (50 mM, 30 s each separated by 30 s) were applied at 10 min intervals. Therefore, cultures were either not stimulated (S0), stimulated once (S1, at 10 min), or stimulated twice (S2, at 10 and 20 min) during this 30 min time period. ***B***, Representative electron micrographs are shown. Scale bar, 500 nm. Black and white arrows indicate HRP-labeled SVs and endosomes, respectively. ***C***, Bar graph displays the mean number of HRP-labeled endosomes per nerve terminal ± SEM (number of independent experiments = 3; one-way ANOVA). ***D***, Frequency distribution of endosome diameter after the 30 min period is shown. At least 140 HRP-labeled endosomes were used for diameter measurements per independent experiment (not significant, two-way ANOVA).

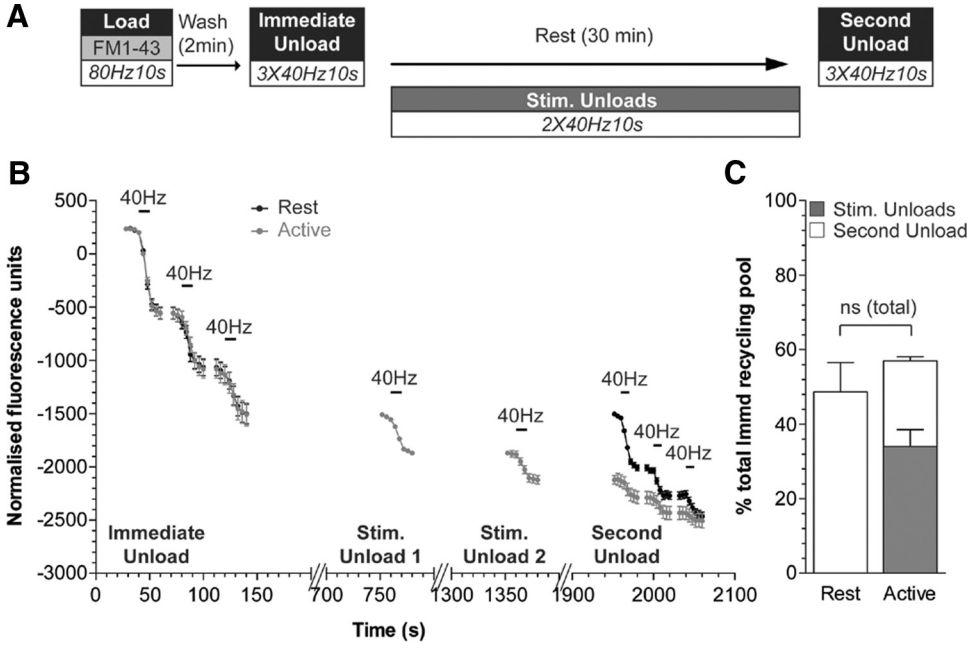

Figure 4. The replenishment of the recycling pool by bulk endosome-derived SVs is independent of activity. ***A***, Cultures were loaded with FM1-43 (10 μM) using a train of 800 action potentials (80 Hz) and washed for 2 min to remove excess dye. The recycling pool was then released using three trains of 400 action potentials (40 Hz, Immediate Unload). The same unloading stimulus was delivered after a 30 min rest period (Second Unload). Where indicated, two additional trains of 400 action potentials (40 Hz) were delivered at 10 min intervals (Stim. Unloads). ***B***, Representative traces in arbitrary fluorescence units are shown for the unloading of FM1-43 in cells without (Rest) or with (Active) additional stimulations during the 30 min rest period. Bars indicate the period of stimulation. ***C***, Mean SV recycling pool sizes after 30 min rest normalized to total immediate recycling pool are shown. The accumulated amount of dye unload during the additional unloading steps was also plotted (gray bar). Number of independent experiments: Rest, 3; Active, 4; all ± SEM, two-tailed Student's *t* test.

SV budding from bulk endosomes is not activity dependent

The previous experiment indicated that SV generation from bulk endosomes requires an increase in $[Ca^{2+}]_i$. SV budding was not affected by the absence of extracellular calcium, suggesting plasma membrane calcium influx was not required for this event. To determine whether activity-dependent calcium influx could facilitate SV budding, we examined bulk endosome dynamics during neuronal activity. HRP-labeled SVs and bulk endosomes were generated using a maximal stimulus as before, and then cultures were left either to rest for 30 min or be subjected to multiple depolarizing stimuli within this 30 min time period (Fig. 3*A*). We reasoned that if neuronal activity was providing calcium

influx for SV budding from bulk endosomes, then more HRP-labeled SVs would be produced in cultures that received additional epochs of activity during the 30 min rest period. Budding events were assessed by monitoring bulk endosome diameter, since new HRP-labeled SVs would be released during neuronal activity, confounding the result. When this protocol was performed, cultures that received additional periods of activity displayed no significant change in either average bulk endosome number (Fig. 3*C*) or the proportion of small endosomes (Fig. 3*D*). This suggests that activity-dependent influx of extracellular calcium cannot facilitate SV budding from bulk endosomes.

To confirm this result, we performed a similar experiment using the fluorescent dye FM1-43, which labels both SVs and bulk endosomes during strong stimulation (Cheung et al., 2010). This approach does allow the quantification of newly generated SVs produced from bulk endosomes, since their release can be monitored as a loss of fluorescence during additional periods of activity. FM1-43 was loaded using a train of high-frequency action potentials (800 at 80 Hz), and then dye-labeled SVs (generated by CME) were immediately depleted using three consecutive action potential trains (Immediate Unload, 400 at 40 Hz; Fig. 4*A*,*B*). To determine the effect of neuronal activity on SV generation from bulk endosomes, cultures were either rested for the 30 min time period or challenged with two additional trains of 400 action potentials delivered at 10 min intervals (Fig. 4*A*). The corresponding loss of fluorescence during this stimulation was measured to quantify the number of releasable SVs (Fig. 4*B*, Stim. Unloads). The total number of SVs generated over the 30 min time period was then quantified by applying three consecutive action potential trains (Second Unload, 400 at 40 Hz) to cultures that were either rested or subjected to additional neuronal activity. The cumulative number of SVs that were generated was not significantly different between the two stimulation conditions (Fig. 4*B*,*C*); therefore, neuronal activity does not impact on SVs generation from bulk endosomes.

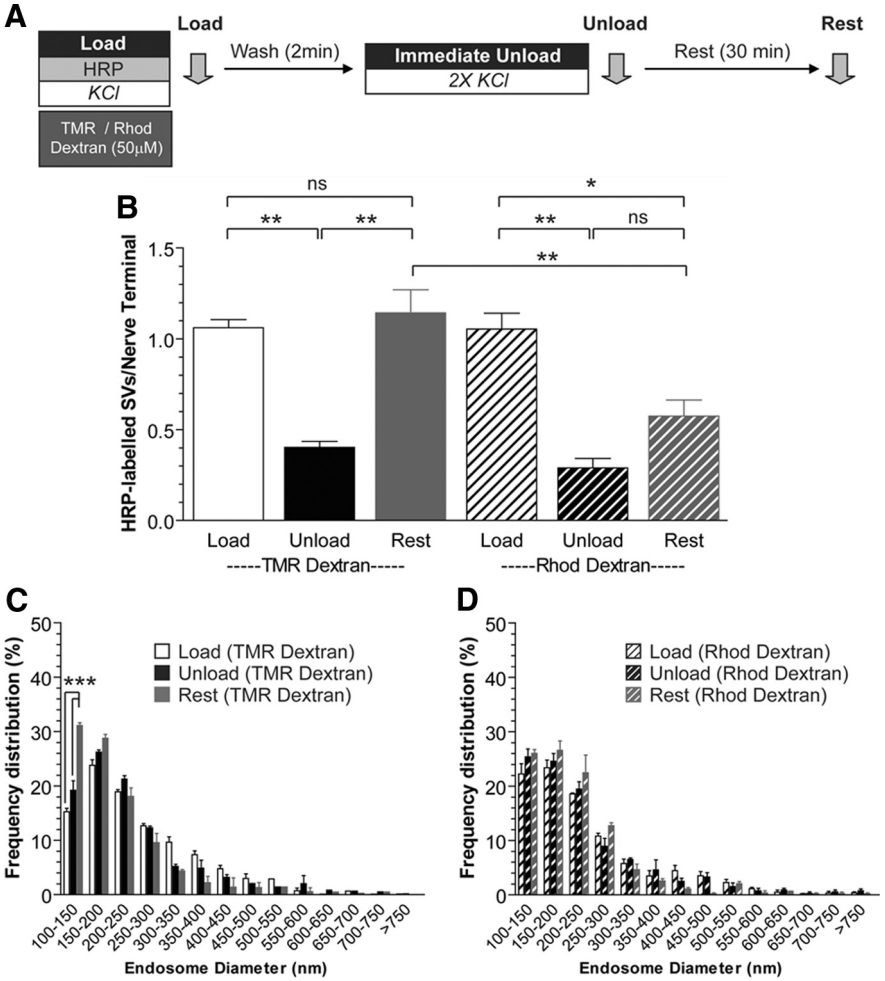

Figure 5. Calcium within bulk endosomes is required for SV budding. ***A***, Cultures were loaded with HRP (10 mg/ml) and either TMR-Dextran (50 μM) or Rhod-Dextran (50 μM) for 2 min in the presence of KCl (50 mM). Cells were washed immediately and then stimulated twice with KCl (50 mM, 30 s each) to release all available SVs (Immediate Unload) and left to rest for 30 min. Cultures were fixed after HRP loading (Load), the immediate unload (Unload), or the rest period (Rest), as indicated by arrows. ***B***, Bar graph displays the mean number of HRP-labeled SVs per nerve terminal ± SEM (number independent experiments = 3 for both; $^{**}p < 0.01$, $^{*}p < 0.05$, one-way ANOVA). ***C***, ***D***, Frequency distribution of endosome diameter for Load, Unload, and Rest in cells loaded with either TMR-Dextran (***C***) or Rhod-Dextran (***D***). At least 70 HRP-labeled endosomes were used for diameter measurements per independent experiment. $^{***}p < 0.001$, two-way ANOVA.

Bulk endosomes are the intracellular calcium source for SV budding

Since extracellular calcium influx did not influence SV generation from bulk endosomes, we next determined whether calcium within the bulk endosome itself was required for SV budding. To test this, we specifically buffered calcium inside bulk endosomes using a high-affinity calcium chelator conjugated to a high-molecular-weight dextran (Rhod-dextran) (Lloyd-Evans et al., 2008). The HRP uptake assay was performed as before, with the exception that Rhod-dextran was coapplied with HRP to ensure that it was internalized inside bulk endosomes in the fluid phase (Fig. 5*A*). This procedure ensured the specific buffering of calcium inside bulk endosomes, since dextrans are too large to be accumulated inside single SVs (Holt et al., 2003; Clayton et al., 2008). As a control, a different high-molecular-weight dextran with no calcium buffering activity [tetramethylrhodamine (TMR)-dextran] was used to ensure that any observed effects were not due to stearic hindrance of SV budding. Inclusion of either Rhod-dextran or TMR-dextran in the fluid phase did not affect the generation of HRP-labeled SVs by CME (0.89 ± 0.02, control; 1.06 ± 0.04, TMR-dextran; 1.05 ± 0.09, Rhod-dextran; $p = 0.146$, one-way ANOVA) or bulk endosomes generated by ADBE (HRP endosomes per nerve terminal; 5.83 ± 0.29, control; 5.77 ± 0.27, TMR-dextran; 5.40 ± 0.29, Rhod-dextran; $p = 0.544$, one-way ANOVA, $n = 3$ experiments). Similarly, the fusion of HRP-labeled SVs during the immediate unload step was not affected by either dextran (Unload; Fig. 5*B*). However, after 30 min a large reduction in the number of newly generated HRP-labeled SVs was observed in neurons containing Rhod-dextran-loaded bulk endosomes (Fig. 5*B*). In contrast, TMR-dextran-loaded neurons generated HRP-labeled SVs from

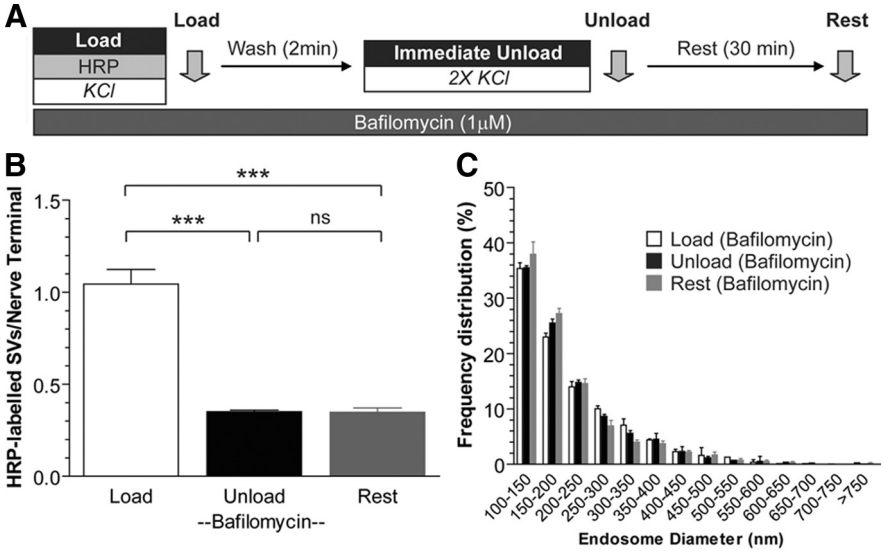

Figure 6. Bulk endosome acidification is required for SV budding. ***A***, Cultures were loaded with HRP (10 mg/ml) for 2 min in the presence of KCl (50 mM) and washed immediately to remove excess HRP. Cultures were then stimulated twice with KCl (50 mM, 30 s each) to release all available SVs (Immediate Unload) and left to rest for 30 min. Bafilomycin A1 (1 μM) was present during the experiment to prevent bulk endosome acidification. Cultures were fixed after HRP loading (Load), the immediate unload (Unload), or the rest period (Rest), as indicated by arrows. ***B***, Bar graph displays the mean number of HRP-labeled SVs per nerve terminal $\pm$SEM (number of independent experiments = 3; ***$p < 0.001$, one-way ANOVA). ***C***, Frequency distribution of endosome diameter for Load, Unload, and Rest in the presence of bafilomycin A1. At least 170 HRP-labeled endosomes were used for diameter measurements per independent experiment (not significant, two-way ANOVA).

bulk endosomes over the same time period (Fig. 5*B*). Rhod-dextran also inhibited the appearance of small HRP-labeled endosomes, in contrast to TMR-dextran-loaded neurones (Fig. 5*C*,*D*). Thus, inclusion of a large-molecular-weight calcium chelator (Rhod-dextran) in the fluid phase during HRP loading arrests SV generation from HRP-labeled bulk endosomes. This suggests that buffering of bulk endosome calcium inhibits SV budding and that fluid phase uptake of extracellular calcium during ADBE is essential for the subsequent generation of SVs.

Bulk endosome acidification is required for SV budding

Studies in non-neuronal cells have shown that intra-endosomal calcium is released during organelle acidification, and that this release is arrested by inhibition of the V-type ATPase using bafilomycin A1 (Gerasimenko et al., 1998). To determine whether this also occurs in bulk endosomes, we acutely inhibited organelle acidification by including bafilomycin A1 at all stages of the HRP uptake assay (Fig. 6*A*). Bafilomycin A1 has no effect on both the exocytosis and endocytosis of SV in cultured neurones (Cousin and Nicholls, 1997; Sankaranarayanan and Ryan, 2001), and, in agreement, application of the drug did not affect HRP loading into either SVs (HRP-labeled SVs per nerve terminal: control, 0.89 $\pm$ 0.02; bafilomycin A1, 1.04 $\pm$ 0.08; $p = 0.14$, two-tailed t test, $n = 3$ experiments) or bulk endosomes (HRP-labeled endosomes per nerve terminal: control, 5.83 $\pm$ 0.29; bafilomycin A1, 5.35 $\pm$ 0.20; $p = 0.24$, two-tailed t test), or the subsequent unloading of HRP (Fig. 6*B*). However, bafilomycin A1 treatment did arrest the generation of HRP-labeled SVs from bulk endosomes (Fig. 6*B*) and retarded the generation of small endosomes (Fig. 6*C*) over the 30 min rest period. Thus, arresting organelle acidification inhibits SV budding from bulk endosomes. This effect was most probably due to the arrest of bulk endosome acidification during the 30 min rest period, since all other aspects of SV recycling were unaffected by bafilomycin.

We have previously shown that bulk endosome-derived SVs specifically replenish the reserve pool of SVs after high-intensity stimulation (Cheung et al., 2010; Cheung and Cousin, 2012). Therefore, we determined whether the potential acidification of bulk endosomes is also required for replenishment of the reserve pool of SVs using a previously validated assay (Cheung et al., 2010). In this assay, both CME and ADBE are triggered with a train of 800 action potentials (80 Hz) in the presence of the dye FM1-43 (Fig. 7*A*). FM1-43-loaded SVs were then depleted immediately after dye loading by sequentially unloading the RRP (60 action potentials at 30 Hz) and then the reserve pool (three trains of 400 action potentials at 40 Hz) (Cheung et al., 2010). Cultures were rested for 30 min to allow SV generation from bulk endosomes and their subsequent replenishment of SV pools. The RRP and reserve pool were then mobilized again, with the majority of released fluorescence originating from the reserve pool (Fig. 7*B*,*C*).

Bafilomycin A1 was applied at all steps of the assay as before and had no effect on either FM1-43 loading or the subsequent unloading of CME-derived SVs (Fig. 7*B*,*C*). However, the subsequent replenishment of the reserve pool was significantly retarded after the 30 min rest period (Fig. 7*B*,*C*). Thus, bafilomycin disrupts both the generation of new SVs from bulk endosomes and their subsequent replenishment of the reserve pool. This suggests that acidification of the bulk endosome may trigger the efflux of accumulated calcium to stimulate SV budding.

Calcineurin activity is essential for SV budding from bulk endosomes

We next determined the identity of the downstream effector for calcium-dependent SV budding from bulk endosomes. We started by examining the role of the calcium-dependent protein phosphatase calcineurin, since it has a previously established role in ADBE (Clayton et al., 2009). First, we performed the HRP uptake assay in cultures that were incubated with the calcineurin antagonist cyclosporin A (CsA; 10 μM) after HRP exposure (and thus endocytosis) was complete (Fig. 8*A*). CsA did not affect the release of HRP-labeled SVs during the immediate unloading stimulation; however, it did abolish the generation of new HRP-labeled SVs during the 30 min rest period (Fig. 8*C*). This inhibition was accompanied by a significant reduction in the population of small HRP-labeled endosomes (Fig. 8*D*). Thus, inhibition of calcineurin arrests the generation of new HRP-labeled SVs from bulk endosomes, suggesting it may be the calcium release sensor from bulk endosomes.

To confirm an essential role for calcineurin in SV generation from bulk endosomes, we examined reserve SV pool replenishment using FM1-43. CsA was applied after loading of FM1-43 with 800 action potentials, to ensure it would not interfere with bulk endosome generation by ADBE (Fig. 9*A*). CsA had no effect on the unloading of either the RRP or the reserve pool during the immediate unloading challenge (Fig. 9*B*,*C*). After the 30 min rest period, however, replenishment of the reserve pool was signifi-

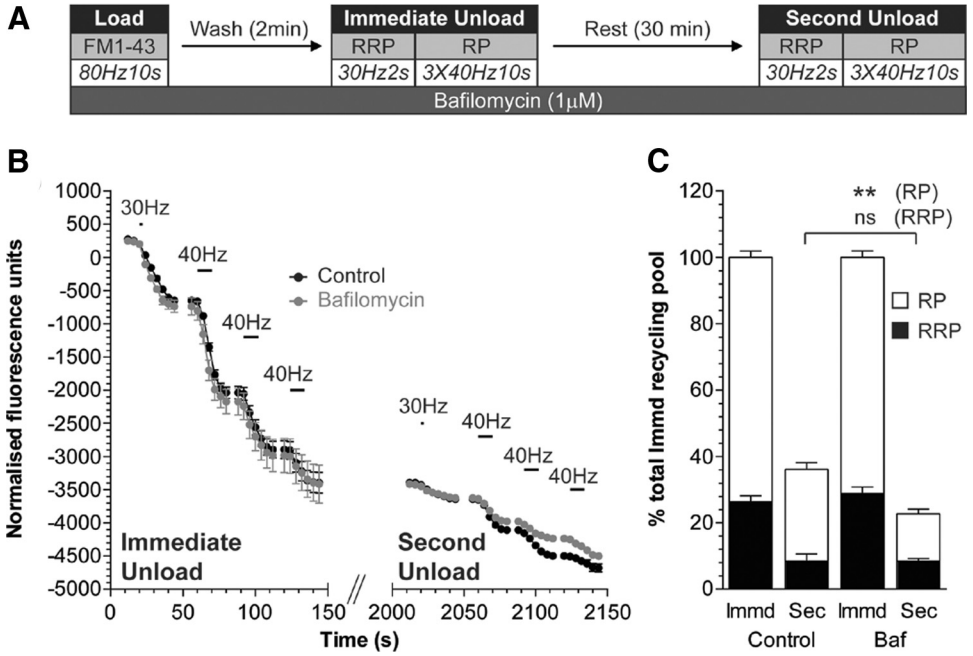

Figure 7. Bulk endosome acidification is required for replenishment of the SV reserve pool. ***A***, Cultures were loaded with FM1-43 (10 μM) using a train of 800 action potentials (80 Hz) and washed for 2 min to remove excess dye. The RRP and reserve pool (RP) were sequentially unloaded using 60 action potentials (30 Hz) followed by three trains of 400 action potentials (40 Hz, Immediate Unload). The same unloading stimuli were delivered after a 30 min rest period (Second Unload). Bafilomycin A1 (1 μM) was added to cultures before dye loading and was present at all steps thereafter. ***B***, Representative traces in arbitrary fluorescence units are shown for the unloading of FM1-43 during both immediate and second unloads (black, control; gray, bafilomycin). Bars indicate the period of stimulation. ***C***, Mean RRP (black bars) and RP (white bars) sizes normalized to the total immediate recycling pool are plotted for both immediate and second unloads ±SEM (number of independent experiments = 3; $^{**}p < 0.01$, one-way ANOVA).

cantly reduced (Fig. 9*C*). Thus, inhibition of SV generation from bulk endosomes by CsA translates into a decreased replenishment of the reserve pool. This highlights that calcineurin is required at multiple calcium-dependent points in the ADBE pathway, in the generation of both bulk endosomes from the plasma membrane and SVs from bulk endosomes.

Discussion

We have shown that calcium accumulated by fluid phase uptake during ADBE is essential for the subsequent generation of SVs from bulk endosomes. We state this since SV budding can be arrested by (1) buffering of $[Ca^{2+}]_i$ by BAPTA-AM, (2) buffering of bulk endosome calcium by Rhod-dextran, (3) inhibition of endosome acidification by bafilomycin A1, and (4) inhibition of the calcium-activated protein phosphatase calcineurin. To our knowledge, this is the first demonstration of a calcium-dependent SV budding event in nerve terminal physiology and highlights the key role calcium plays in multiple steps of the SV life cycle during high-intensity stimulation.

The majority of the work performed in this study used a recently characterized morphological assay that specifically tracks SVs generated by ADBE (Cheung and Cousin, 2012). Crucially, this assay allowed the role of calcium in SV budding to be decoupled from other aspects of the SV life cycle including exocytosis, CME, and bulk endosome generation by ADBE. Furthermore, this assay is direct and does not require further stimulation to report SV generation. The nature of the assay requires multiple stimuli to be delivered to cultures over a prolonged time course. Because of this, KCl was used both to evoke ADBE and to deplete HRP-loaded SVs. We have shown previously that application of elevated KCl is equivalent to the delivery of 800 action potentials (80 Hz) in terms of the extent of SV exocytosis evoked (Cousin and Evans, 2011); the amount of ADBE and CME triggered (Clayton et al., 2009) and the replenishment of both the RRP and reserve pools (Cheung and Cousin, 2012). Where possible, we also used a reserve pool replenishment assay to corroborate our results, since ADBE-derived SVs selectively refill this pool (Richards et al., 2000; Cheung et al., 2010; Cheung and Cousin, 2012). This assay requires stimulation to quantify the number of SVs produced by ADBE, and therefore its output is confounded by treatments that modulate SV exocytosis (e.g., chelation of intracellular calcium with BAPTA-AM), explaining why its use has been limited to specific experiments in this study.

The key observation from this work is that a store of calcium within bulk endosomes is required for SV generation from this organelle. A role for calcium in endosome function has been suggested before, where the *in vitro* fusion of classical early endosomes purified from neuroendocrine cells was arrested by buffering of either extra- or intra-endosomal calcium via application of extracellular BAPTA or EGTA-AM, respectively (Holroyd et al., 1999; Rizzoli et al., 2006). Similarly, there is increasing interest in calcium release from endolysosomal structures as part of a second messenger cascade. In these systems, the proton-motive force of the organelle is required to accumulate calcium for subsequent release triggered by NAADP (nicotinic acid adenine dinucleotide phosphate) (Morgan et al., 2011). Both of the examples described above contrast with our study, since calcium is directly accumulated inside bulk endosomes during fluid phase uptake and then released on endosome acidification. Evidence for a similar mechanism exists in non-neuronal cells, where extracellular calcium accumulated by fluid phase uptake is released from either endosomes or phagosomes on their acidification (Gerasimenko et al., 1998; Lundqvist-Gustafsson et al., 2000); however, little is known regarding the function of this efflux. Our demonstration of a

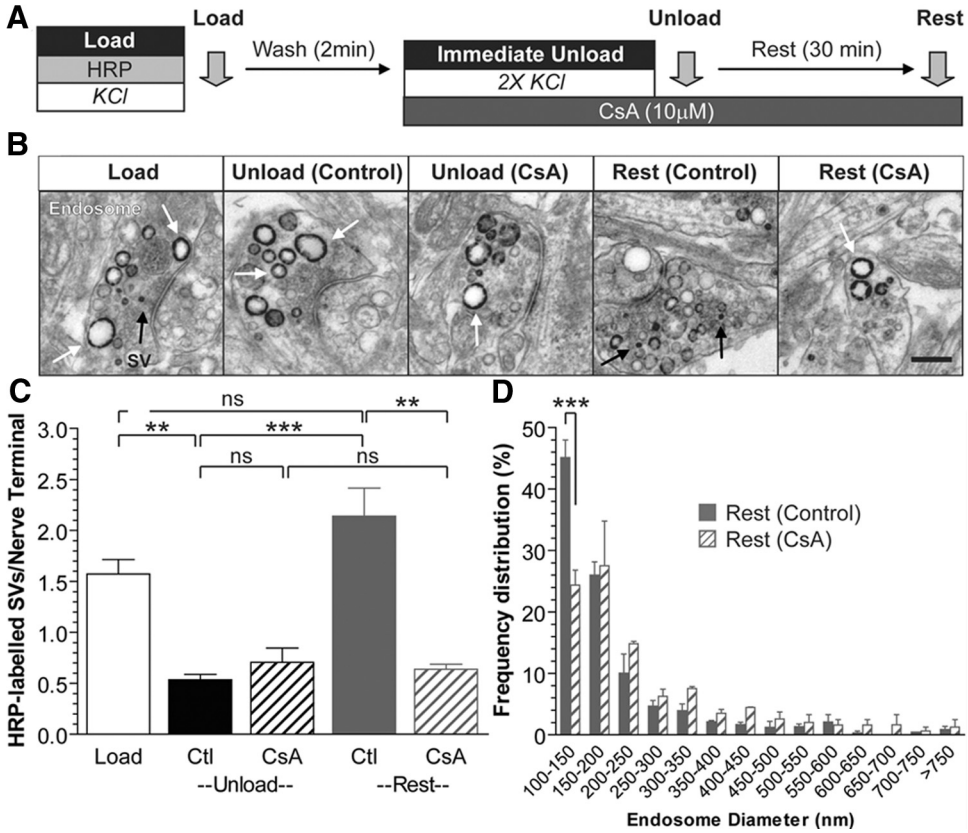

Figure 8. Calcineurin activity is essential for SV budding from bulk endosomes. ***A***, Cultures were loaded with HRP (10 mg/ml) for 2 min in the presence of KCl (50 mM) and washed immediately to remove excess HRP. Cells were then stimulated twice with KCl (50 mM, 30 s each) to release all available SVs (Immediate Unload) and left to rest for 30 min. CsA (10 μM) was added during the KCl unload and also the rest period. Cultures were fixed after HRP loading (Load), the immediate unload (Unload), or the rest period (Rest), as indicated by arrows. ***B***, Representative electron micrographs are shown. Scale bar, 500 nm. Black and white arrows indicate HRP-labeled SVs and endosomes, respectively. ***C***, Bar graph displays the mean number of HRP-labeled SVs per nerve terminal ±SEM (number of independent experiments: Load, 5; Unload-Control, 3; Unload-CsA, 3; Rest-Control, 3; Rest-CsA, 3; $^{***}p < 0.001$, $^{**}p < 0.01$, one-way ANOVA). ***D***, Frequency distribution of endosome diameter after Rest in the presence or absence of CsA. At least 130 HRP-labeled endosomes were used for diameter measurements per independent experiment. $^{***}p < 0.001$, two-way ANOVA.

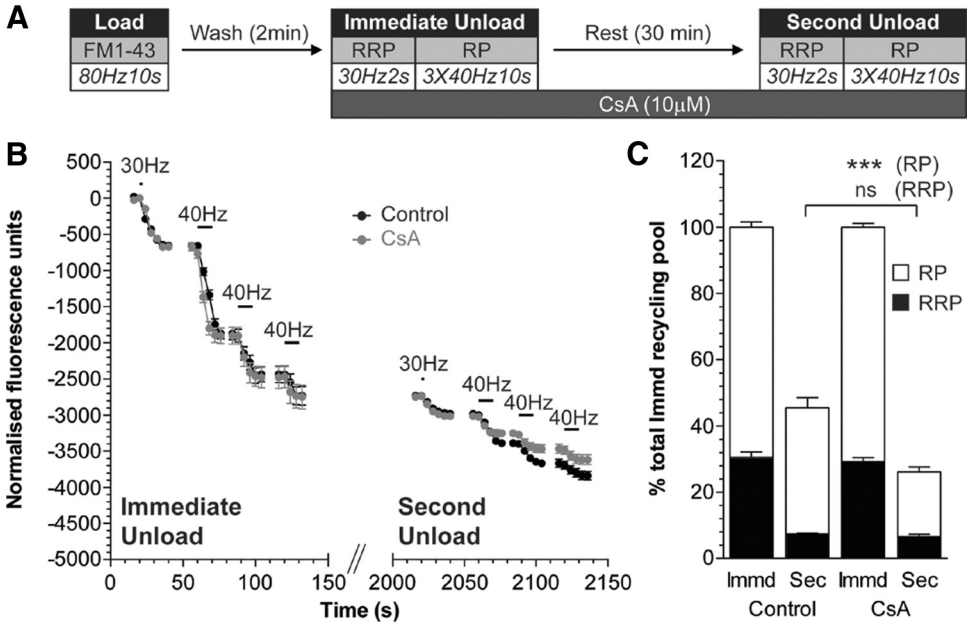

Figure 9. Cyclosporin A inhibits the replenishment of SV reserve pool via bulk endosomes. ***A***, Cultures were loaded with FM1-43 (10 μM) using a train of 800 action potentials (80 Hz) and washed for 2 min to remove excess dye. The RRP and reserve pool (RP) were sequentially unloaded using 60 action potentials (30 Hz) followed by three trains of 400 action potentials (40 Hz, Immediate Unload). The same unloading stimuli were delivered after a 30 min rest period (Second Unload). CsA (10 μM) was added to cultures before the Immediate Unload and was present thereafter. ***B***, Representative traces in arbitrary fluorescence units are shown for the unloading of FM1-43 during both immediate and second unloads (black, control; gray, CsA). Bars indicate the period of stimulation. ***C***, Mean RRP (closed bars) and RP (open bars) sizes normalized to the total immediate recycling pool are plotted for both immediate and second unloads ±SEM (number of independent experiments; Control, 3; CsA, 4; $^{***}p < 0.001$, one-way ANOVA).

key role for this endosomal calcium store in SV generation suggests a potential for parallel calcium-dependent vesicle processing events in other biological systems.

Inhibition of endosomal acidification with bafilomycin A1 arrests calcium efflux from endosomes in non-neuronal cells (Gerasimenko et al., 1998). Interestingly, a reduction in the level of extracellular calcium resulted in a retardation of endosomal acidification, suggesting a reciprocal relationship between calcium uptake and the creation of a pH gradient (Gerasimenko et al., 1998). We attempted to visualize calcium efflux from bulk endosomes using cytosolic indicators; however, due to the highly localized nature of these increases, no signal was observed. Therefore, while experimental evidence indicates that bulk endosome acidification results in the efflux of stored calcium, we do not have a direct demonstration of this event. Regardless, our study still reveals a novel role for organelle acidification in the generation of SVs in central nerve terminals.

The role of calcineurin in the SV life cycle has been investigated extensively, with the phosphatase proposed to control multiple aspects including ADBE (Evans and Cousin, 2007; Clayton et al., 2009), CME (Sun et al., 2010), SV distribution between the recycling and resting pools (Kim and Ryan, 2010), and even kiss-and-run (Samasilp et al., 2012). The arrest of SV budding from bulk endosomes during calcineurin inhibition reveals another essential requirement for this enzyme in the ADBE retrieval pathway. For calcineurin to be activated by bulk endosome calcium, it must be anchored in close proximity to these organelles. One potential mechanism for calcineurin localization is an interaction with the dynamin I xb splice variant, which possesses a calcineurin interaction motif at its extreme C terminus (Bodmer et al., 2011; Xue et al., 2011). This interaction is essential for dynamin I dephosphorylation and subsequent bulk endosome generation (Xue et al., 2011). Work from our laboratory indicates that dynamin is required for SV generation from bulk endosomes (G.C., unpublished observations), suggesting that calcineurin should be in the correct location to encounter calcium release from these organelles.

An outstanding question is, what is the calcineurin substrate that mediates SV generation from bulk endosomes? Calcineurin dephosphorylates a group of endocytosis proteins called dephosphins during nerve terminal stimulation (Cousin and Robinson, 2001). Of this group, a potential substrate may be dynamin I, which binds calcineurin (Bodmer et al., 2011; Xue et al., 2011) and whose dephosphorylation recruits the F-BAR protein syndapin I (Anggono et al., 2006). Syndapin plays an essential role in vesicle generation from endosomes in non-neuronal cells via interactions with EHD proteins (Braun et al., 2005), suggesting a possible downstream mechanism for SV generation in central nerve terminals. Alternatively, dephosphorylation of the lipid phosphatase synaptojanin or the lipid kinase PIP kinase 1γ may be required for SV generation, since PI(4,5)P_2 metabolism is an essential step in multiple trafficking pathways, albeit usually at the plasma membrane (Haucke and Di Paolo, 2007). Another potential candidate is AP180 (Cousin et al., 2001), which may be recruited to aid AP-1/AP-3-dependent SV budding (Cheung and Cousin, 2012). Whether multiple dephosphorylation events are required, or dephosphorylation of a single substrate, are questions currently under investigation in our laboratory.

We have revealed a key molecular step in ADBE, an SV retrieval mode that is dominant during intense neuronal activity (Clayton et al., 2008). This calcium-dependent SV budding event is, to our knowledge, the first demonstration of a role for fluid phase calcium uptake in the SV life cycle, suggesting that its modulation may impact on physiological and pathophysiological events such as memory generation and epilepsy.

References

Anggono V, Smillie KJ, Graham ME, Valova VA, Cousin MA, Robinson PJ (2006) Syndapin I is the phosphorylation-regulated dynamin I partner in synaptic vesicle endocytosis. Nat Neurosci 9:752–760. CrossRef Medline

Bodmer D, Ascaño M, Kuruvilla R (2011) Isoform-specific dephosphorylation of dynamin1 by calcineurin couples neurotrophin receptor endocytosis to axonal growth. Neuron 70:1085–1099. CrossRef Medline

Braun A, Pinyol R, Dahlhaus R, Koch D, Fonarev P, Grant BD, Kessels MM, Qualmann B (2005) EHD proteins associate with syndapin I and II and such interactions play a crucial role in endosomal recycling. Mol Biol Cell 16:3642–3658. CrossRef Medline

Cheung G, Cousin MA (2012) Adaptor protein complexes 1 and 3 are essential for generation of synaptic vesicles from activity-dependent bulk endosomes. J Neurosci 32:6014–6023. CrossRef Medline

Cheung G, Jupp OJ, Cousin MA (2010) Activity-dependent bulk endocytosis and clathrin-dependent endocytosis replenish specific synaptic vesicle pools in central nerve terminals. J Neurosci 30:8151–8161. CrossRef Medline

Clayton EL, Evans GJ, Cousin MA (2008) Bulk synaptic vesicle endocytosis is rapidly triggered during strong stimulation. J Neurosci 28:6627–6632. CrossRef Medline

Clayton EL, Anggono V, Smillie KJ, Chau N, Robinson PJ, Cousin MA (2009) The phospho-dependent dynamin-syndapin interaction triggers activity-dependent bulk endocytosis of synaptic vesicles. J Neurosci 29:7706–7717. CrossRef Medline

Cousin MA, Evans GJ (2011) Activation of silent and weak synapses by cAMP-dependent protein kinase in cultured cerebellar granule neurons. J Physiol 589:1943–1955. CrossRef Medline

Cousin MA, Nicholls DG (1997) Synaptic vesicle recycling in cultured cerebellar granule cells: role of vesicular acidification and refilling. J Neurochem 69:1927–1935. Medline

Cousin MA, Robinson PJ (2001) The dephosphins: dephosphorylation by calcineurin triggers synaptic vesicle endocytosis. Trends Neurosci 24:659–665. CrossRef Medline

Cousin MA, Tan TC, Robinson PJ (2001) Protein phosphorylation is required for endocytosis in nerve terminals. Potential role for the dephosphins dynamin I and synaptojanin, but not AP180 or amphiphysin. J Neurochem 76:105–116. Medline

Evans GJ, Cousin MA (2007) Activity-dependent control of slow synaptic vesicle endocytosis by cyclin-dependent kinase 5. J Neurosci 27:401–411. CrossRef Medline

Gerasimenko JV, Tepikin AV, Petersen OH, Gerasimenko OV (1998) Calcium uptake via endocytosis with rapid release from acidifying endosomes. Curr Biol 8:1335–1338. CrossRef Medline

Granseth B, Odermatt B, Royle SJ, Lagnado L (2006) Clathrin-mediated endocytosis is the dominant mechanism of vesicle retrieval at hippocampal synapses. Neuron 51:773–786. CrossRef Medline

Grynkiewicz G, Poenie M, Tsien RY (1985) A new generation of Ca2+ indicators with greatly improved fluorescence properties. J Biol Chem 260:3440–3450. Medline

Haucke V, Di Paolo G (2007) Lipids and lipid modifications in the regulation of membrane traffic. Curr Opin Cell Biol 19:426–435. CrossRef Medline

Heerssen H, Fetter RD, Davis GW (2008) Clathrin dependence of synaptic-vesicle formation at the Drosophila neuromuscular junction. Curr Biol 18:401–409. CrossRef Medline

Holroyd C, Kistner U, Annaert W, Jahn R (1999) Fusion of endosomes involved in synaptic vesicle recycling. Mol Biol Cell 10:3035–3044. Medline

Holt M, Cooke A, Wu MM, Lagnado L (2003) Bulk membrane retrieval in the synaptic terminal of retinal bipolar cells. J Neurosci 23:1329–1339. Medline

Kasprowicz J, Kuenen S, Miskiewicz K, Habets RL, Smitz L, Verstreken P (2008) Inactivation of clathrin heavy chain inhibits synaptic recycling but allows bulk membrane uptake. J Cell Biol 182:1007–1016. CrossRef Medline

Kim SH, Ryan TA (2010) CDK5 serves as a major control point in neurotransmitter release. Neuron 67:797–809. CrossRef Medline

Lloyd-Evans E, Morgan AJ, He X, Smith DA, Elliot-Smith E, Sillence DJ,

Churchill GC, Schuchman EH, Galione A, Platt FM (2008) Niemann-Pick disease type C1 is a sphingosine storage disease that causes deregulation of lysosomal calcium. Nat Med 14:1247–1255. CrossRef Medline

Lundqvist-Gustafsson H, Gustafsson M, Dahlgren C (2000) Dynamic Ca(2+)changes in neutrophil phagosomes A source for intracellular ca(2+)during phagolysosome formation? Cell Calcium 27:353–362. CrossRef Medline

Morgan AJ, Platt FM, Lloyd-Evans E, Galione A (2011) Molecular mechanisms of endolysosomal Ca2+ signalling in health and disease. Biochem J 439:349–374. CrossRef Medline

Richards DA, Guatimosim C, Betz WJ (2000) Two endocytic recycling routes selectively fill two vesicle pools in frog motor nerve terminals. Neuron 27:551–559. CrossRef Medline

Rizzoli SO, Betz WJ (2005) Synaptic vesicle pools. Nat Rev Neurosci 6:57–69. CrossRef Medline

Rizzoli SO, Bethani I, Zwilling D, Wenzel D, Siddiqui TJ, Brandhorst D, Jahn R (2006) Evidence for early endosome-like fusion of recently endocytosed synaptic vesicles. Traffic 7:1163–1176. CrossRef Medline

Samasilp P, Chan SA, Smith C (2012) Activity-dependent fusion pore expansion regulated by a calcineurin-dependent dynamin-syndapin pathway in mouse adrenal chromaffin cells. J Neurosci 32:10438–10447. CrossRef Medline

Sankaranarayanan S, Ryan TA (2001) Calcium accelerates endocytosis of vSNAREs at hippocampal synapses. Nat Neurosci 4:129–136. CrossRef Medline

Sun T, Wu XS, Xu J, McNeil BD, Pang ZP, Yang W, Bai L, Qadri S, Molkentin JD, Yue DT, Wu LG (2010) The role of calcium/calmodulin-activated calcineurin in rapid and slow endocytosis at central synapses. J Neurosci 30:11838–11847. CrossRef Medline

Wu XS, McNeil BD, Xu J, Fan J, Xue L, Melicoff E, Adachi R, Bai L, Wu LG (2009) Ca(2+) and calmodulin initiate all forms of endocytosis during depolarization at a nerve terminal. Nat Neurosci 12:1003–1010. CrossRef Medline

Xue J, Graham ME, Novelle AE, Sue N, Gray N, McNiven MA, Smillie KJ, Cousin MA, Robinson PJ (2011) Calcineurin selectively docks with the dynamin Ixb splice variant to regulate activity-dependent bulk endocytosis. J Biol Chem 286:30295–30303. CrossRef Medline

Zhu Y, Xu J, Heinemann SF (2009) Two pathways of synaptic vesicle retrieval revealed by single-vesicle imaging. Neuron 61:397–411. CrossRef Medline